Liquid Crystals in Novel Geometries prepared by Microfluidics and Electrospinning

Hsin-Ling Liang[a], Eva Enz[a], Giusy Scalia[b] and Jan Lagerwall[a,b]*

[a]Martin-Luther Universität Halle-Wittenberg, Institute of Chemistry - Physical Chemistry, Von-Danckelmannplatz 4, 06120 Halle, Germany

and

[b]Seoul National University, Graduate School of Convergence Science & Technology 864-1, Iui-dong, Yeongtong-gu, 443-270 Suwon-si, Gyeonggi-do, South Korea

**Corresponding author: jan.lagerwall@lcsoftmatter.com*

Abstract: We describe two new techniques of preparing liquid crystal samples and discuss their potential for novel research and applications. Very thin polymer composite fibers functionalized by a liquid crystalline core are realized by coaxial electrospinning of a polymer solution surrounding the liquid crystal during the spinning process. The resulting fiber mats exhibit the special properties and responsiveness of the liquid crystal core, e.g. temperature dependent selective reflection when a short-pitch cholesteric is encapsulated. In the second approach an axisymmetric nested capillary microfluidics set-up is used to prepare liquid crystalline shells suspended in an aqueous continuous phase. The spherical geometry of the shell imposes specific defect configurations, the exact result depending on the prevailing liquid crystal phase, the director anchoring conditions at the inner and outer surfaces, and the homogeneity of the shell thickness. With planar director anchoring a variety of defect configurations are possible but for topological reasons the defects must always sum up to a total defect strength of $s = +2$. Homeotropic anchoring instead gives a defect-free shell, in contrast to a droplet with homeotropic boundary conditions, which must have a defect at its core. By varying the inner and outer fluids as well as the liquid crystal material and temperature, the defect configuration can be tuned in a way that makes the shells interesting e.g. as a versatile colloid crystal building block.

1. Introduction

Liquid crystals (LCs) are traditionally studied in flat display-like samples although they are perfectly compatible also with a variety of other geometries, many of which are so far little explored. Their functionality may be put to use in new ways, possibly with unique features, by preparing liquid crystals in cylindrical, spherical or other morphologies. In this paper we present two approaches toward realizing such samples: electrospun LC-filled nano-/microfibers and microfluidics-produced LC shells. These novel geometries for liquid crystals have potential for application in fields ranging from smart textiles to colloidal crystal design, but also many fascinating non-applied scientific questions arise from their study.

In electrospinning a very thin polymer fiber is produced by applying a strong electric field between a grounded collector and an electrically charged spinneret, to which a polymer solution is slowly pumped [1-3]. The field induced a separation of ions in the solution which for sufficient field strength leads to electrostatic forces stronger than the surface tension, such that a thin jet is expelled from the solution droplet exiting the spinneret. Because the highly charged jet experiences electrostatic self repulsion a bending and whipping instability initiates soon after the jet leaves the spinneret, leading to a dramatic stretching and thinning of the fiber. The fiber that finally lands on the collector can thus be extremely thin and its structure can be made quite complex by using different variations of the basic electrospinning technique.

We use coaxial electrospinning to prepare composite fibers with a core of LC inside a polymer sheath [4-6]. The resulting fibers constitute an entirely new configuration for studying and applying LCs. The LC gives the fibers new functionality and responsiveness and the encapsulation of the LC allows easy investigation of 1D confinement effects. We have so far explored the encapsulation of achiral nematics [4], smectics [5] and, most recently, short-pitch cholesteric and blue phases [6].

Liquid crystal shells are produced by flowing the liquid crystal as the middle fluid between inner and outer fluid phases that are both immiscible with the liquid crystal, typically aqueous surfactant or polymer solutions. We follow a method established in the group of David Weitz [7] for controlled fabrication of the shells using an axisymmetric nested glass capillary microfluidics set-up. The shell morphology is interesting e.g. because of the analogies with lipid membrane vesicles, thanks to which studies of the shells may shed light on processes in biology related to liquid crystal phase transitions that are not yet fully understood [8]. Moreover, the topological defects in spherical liquid crystal shells with tangential director field could render them highly interesting colloidal particles [9]. In our work we focus particularly on smectic phases and phase transitions in the shells.

2. Experimental

In both types of experiment the flows of all fluids are controlled by a 4-channel pressure-driven microfluidics control unit (Fluigent, Paris, France). Compared to standard syringe pumps this has the advantages of faster response to flow rate changes, possibility to work with very small sample volume, and greater flexibility regarding fluid temperature control. Our coaxial electrospinning setup is shown in Fig. 1. The liquid crystal is pumped through a thin flexible capillary that is inserted concentrically into a larger tube through which the polymer solution is pumped. As long as the two fluids are immiscible, which is the case for a thermotropic liquid crystal pumped inside an aqueous or ethanol-based polymer solution, the coaxial geometry can be stable throughout the spinning process until the solvent of the sheath solution has evaporated, leaving a stable composite fiber with the liquid crystal in the core.

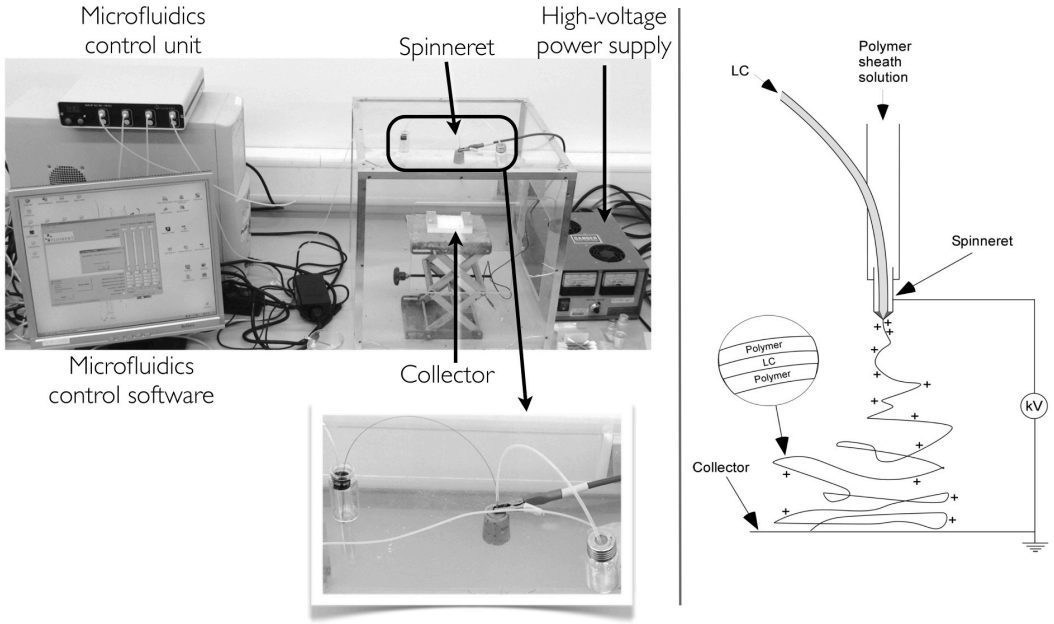

Fig. 1. Our set-up for coaxial electrospinning (left) and a schematic drawing illustrating the process. Reproduced from [10].

In the electrospinning work discussed in this paper we spun a cholesteric (N*) liquid crystal as the core fluid inside a solution of poly(vinylpyrrolidone)- PVP- in ethanol. The liquid crystal was a binary mixture (in the following referred to as **mixture 1**) of the commonly used chiral dopant CB15 and the commercial nematic mixture RO-TN-403/015 S (Roche) at a 50/50 mass ratio. The resulting phase sequence is N* 28.5 BP* 30.2 Iso. / °C.

The microfluidic set-up for producing the liquid crystal shells, adapted from the design of the Weitz group [7], is shown in Fig. 2. In the experiments described in this paper the inner and outer fluids are both aqueous solutions of the nonionic polymeric surfactant Pluronic F127 (5% by weight), cf. Fig. 3. The inner fluid is pumped through a tapered cylindrical capillary that is fitted axisymmetrically into a square capillary. The liquid crystal, here the well known material 8CB (Crystal 21.5 SmA 33.5 N 41.5 Iso. /°C), is pumped into this capillary such that it flows around the former capillary, eventually enveloping the inner fluid after the tapered orifice. From the other direction in the same square capillary the outer fluid is flown. Since it is immiscible with the liquid crystal the stream of 8CB with contained inner fluid is flow-focused into small shells dispersed in the outer fluid, and the resulting colloid is collected in a second tapered cylindrical capillary which is also fitted into the square capillary, but from the other direction. In our set-up temperature control is added where needed in order to take the liquid crystal to its isotropic phase during the shell formation process.

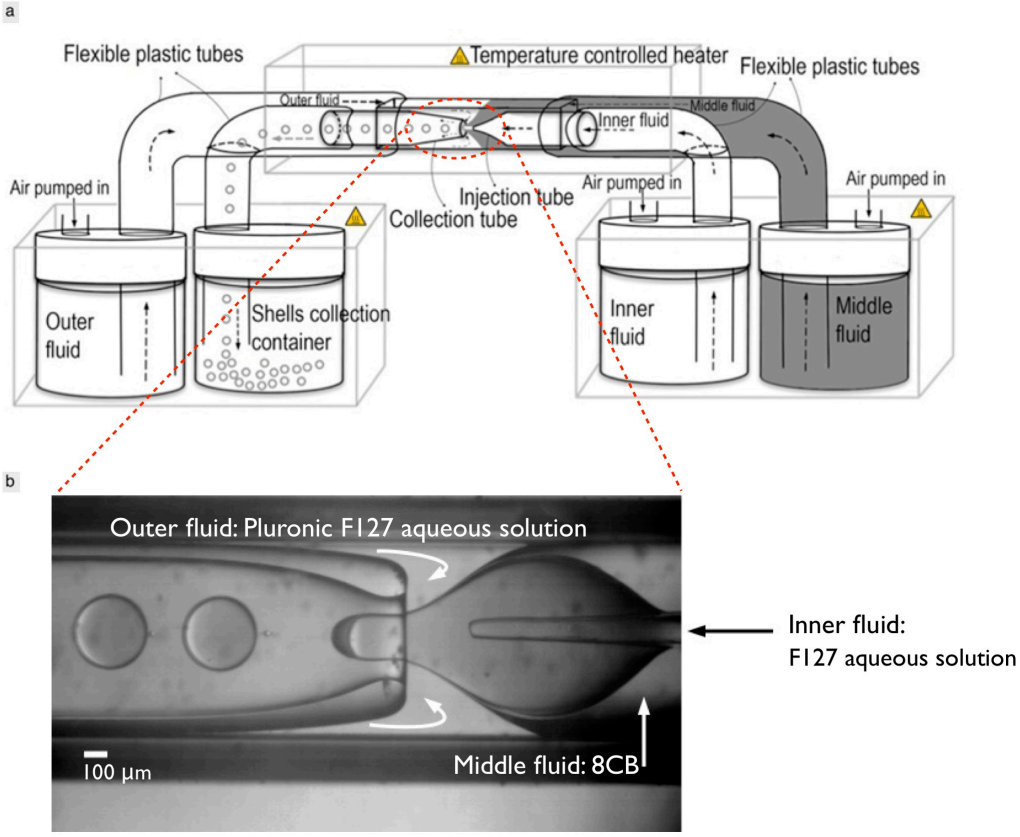

Fig. 2. (a) Schematic diagram and (b) high-speed video optical microscopy image of 8CB spherical shells generated in our capillary microfluidic device system. Reproduced from [11].

The interfaces between the liquid crystal and the inner and outer aqueous phases, respectively, were stabilized by the F127 surfactant. F127 is a predominantly hydrophilic amphiphilic triblock co-polymer, with the approximate formula PEO_{99}-PPO_{67}-PEO_{99}, where PEO and PPO

denote poly(ethylene oxide) and poly(propylene oxide), respectively [12]. It is fully hydrated at low temperatures including room temperature, but upon heating many of the hydrogen bonds between the polymer and the water molecules are broken, leading to increasing hydrophobicity at higher temperatures [13]. This has the effect that the polymer forms a random coil structure at low temperatures whereas it aggregates into micelles, with hydrophobic PPO core, at higher temperatures. The resulting critical micelle temperature (CMT), i.e. the limit between coil unimers at low temperatures and micelles at high temperatures was found to be about 20°C at the F127 concentration employed here [14]. Within the liquid crystal temperature range of the 8CB shell the polymers should thus be present predominantly as micelles.

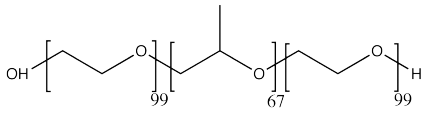

Fig. 3. Chemical structure of the nonionic polymer surfactant Pluronic F127.

3. Results and Discussion

3.1 Electrospinning

The selectively reflecting short-pitch cholesteric liquid crystal encapsulated in the fibers gives them the color of the liquid crystal, visibly even macroscopically in case of well-filled fibers, as shown in [6]. The confinement in the narrow fiber core, together with the planar alignment along the fiber axis induced at the inside of the sheath, however creates strong constraints on the helical pitch of the cholesteric. This means that the selectively reflected color is quantized, the wavelength difference between adjacent colors being greater the thinner the fiber. In fact, for fibers thinner than 1 micron only one color is possible, set by the fiber diameter regardless of what the natural pitch of the bulk cholesteric is. For this reason we saw fibers reflecting in red, green or any other color, although the natural color of the liquid crystal is blue. As demonstrated in [6] the change in color can in fact be used to calculate the inner diameter, which was found to vary between 500 and 800 nm depending on the spinning conditions.

The outer diameter was estimated by optical microscopy in [6] to be in the range 1 - 7 microns. Here we additionally present transmission electron microscopy images of some of the thinner fibers, cf. Fig. 4, providing much more accurate diameter data as well as information on the fiber morphology. As can be seen in the figure the liquid crystal-filled fibers are mainly smooth and of cylindrical shape. The diameter is about 1 micron, increasing with increasing amount of liquid crystal filling. Interestingly, the fiber without liquid crystal filling (Fig. 4a) appears collapsed, suggesting that it was initially hollow. It thus seems that the presence of the inner capillary, although no fluid was pumped through it, was sufficient to ensure the initial tubular shape of the polymer sheath, although it collapsed during the process. Also in the cases that liquid crystal was pumped through the inner capillary, a few fibers ended up unfilled. These generally collapsed into quasi-flat ribbons, as seen in Fig. 4d (fiber closest to substrate).

The fibers with cholesteric core hold large potential for wearable sensor applications with simple read-out and without the need for a power source. Because the helical pitch and thus the color of the liquid crystal depends on the encapsulation geometry any induced change to this will result in a color change response. The pitch also responds to chemical changes to the cholesteric liquid crystal which makes it useful for gas sensing [15]. The fact that the sheath can be permeable for various gases, further enhancement being possible by making the sheath porous [16], and the exceptional surface-to-volume ratio of the electrospun fiber samples,

render the N*-functionalized fibers promising as basis for a new class of gas sensors. Our current research efforts aim to explore this potential.

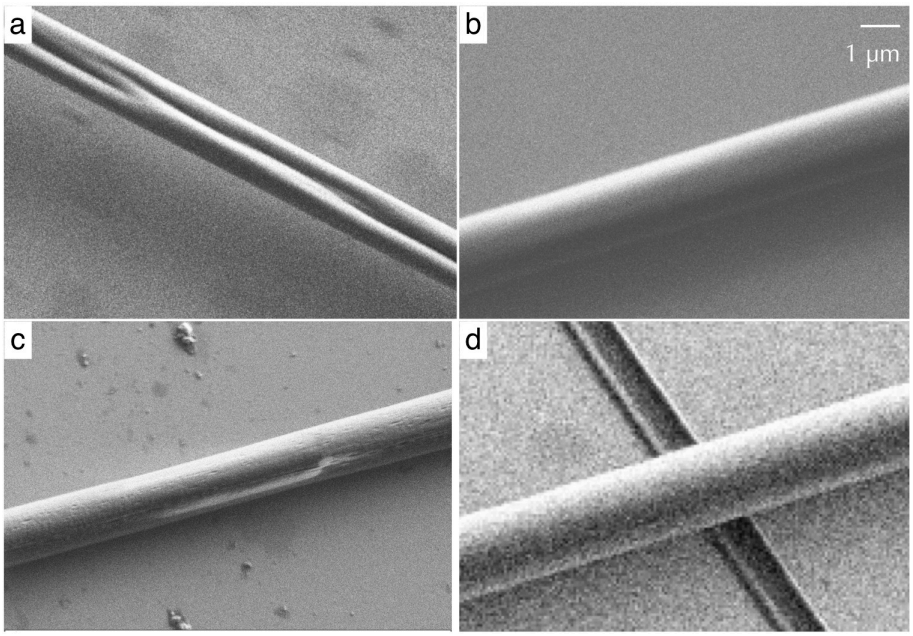

Fig. 4. Scanning electron microscopy images of PVP fibers, empty (a) and with liquid crystal core (b-d). The scale is constant throughout all images (scale bar in b). All samples were spun at room temperature, with 25-35% relative humidity, 10 cm spinneret – collector distance and 10 kV spinning voltage, with a 12.5% PVP in ethanol solution as the outer fluid. This was pumped at a flow rate of 1.8 mL/h in all samples. The inner fluid was **mixture 1**, cholesteric at room temperature, and this was pumped at flow rates of 0.14 mL/h (b), 0.26 mL/h (c) and 0.36 mL/h (d). Reproduced from [10].

3.2 Microfluidics

We studied the polarizing microscopy texture of the 8CB shells during cooling from the isotropic phase, through the nematic and into the SmA phase. The texture at high temperatures of the nematic phase (Fig. 5a) revealed that the director here aligned radially, i.e. the liquid crystal adopted homeotropic alignment. In this geometry the shell is entirely defect-free, in contrast to a homeotropically aligned droplet, which must contain a defect at the center. The shell appears very similar to a typical conoscopy image of a regular flat homeotropic sample, with a black cross and a series of concentric rings varying in color. This is not surprising because optically the situation is in fact totally analogous, it is only the experimental parameters that have been reversed. While we in a conoscopy experiment probe all possible light propagation directions for a single orientation of the director (and thus the optic axis), we here probe all possible director orientations for a single direction of light propagation.

As the shell is cooled down towards the transition to the SmA phase we were surprised to find a dramatic change in texture, reflecting a reorientation of the internal shell structure from homeotropic to planar just before the positional order of the smectic phase takes over, cf. Fig. 5b-g. The process starts as a twisting of the previously well-defined cross into a spiral pattern growing out from the center (b-d). The handedness is random, as expected considering the lack of chiral molecules in the system. This can be verified in Fig. 6 where two shells with the pattern twisting in opposite senses are pictured.

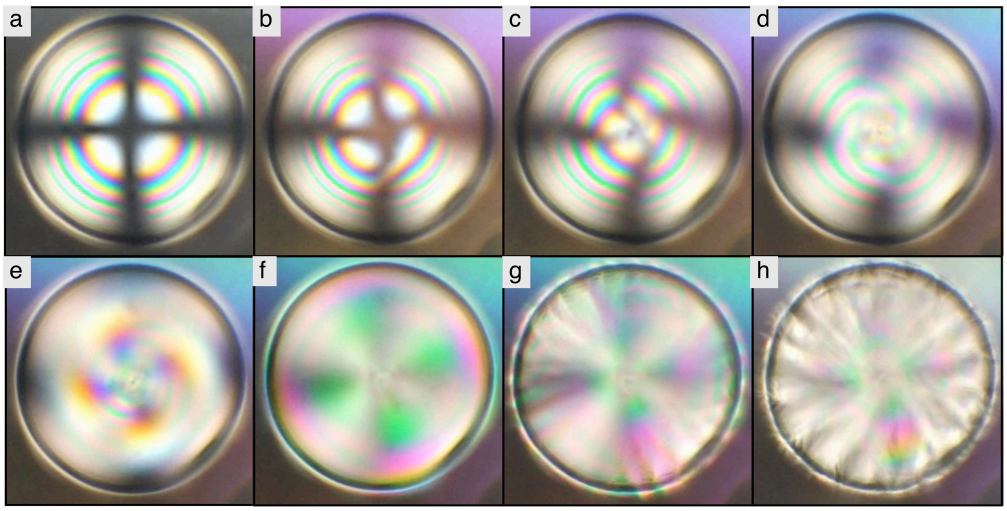

Fig. 5. The polarizing microscopy textures during the change from homeotropic to planar alignment connected to the N-SmA transition. The shell diameter is about 170 μm, the thickness about 10 μm.

The (repeatable) change from homeotropic to planar alignment upon cooling shows that the energy of planar alignment becomes lower than that of homeotropic at temperatures close to the N-SmA transition, whereas it is the other way around at higher temperatures (on heating, the reverse alignment change takes place). As a change from homeotropic to planar alignment involves a substantial reorganization of the shell's internal structure the two energy minima must be separated by a non-negligible energy barrier. A possible interpretation of the textural evidence is the following. As we cool down to below the temperature where planar alignment gives a deeper energy minimum, thermal fluctuations first overcome the energy barrier at a point very close to the top of the shell (below we will explain why it occurs here first), where the director thus reorients by 90 degrees, producing an intermediate twisted director geometry. The realignment then spreads around the shell in a 'domino effect' style process, giving rise to the spiral pattern.

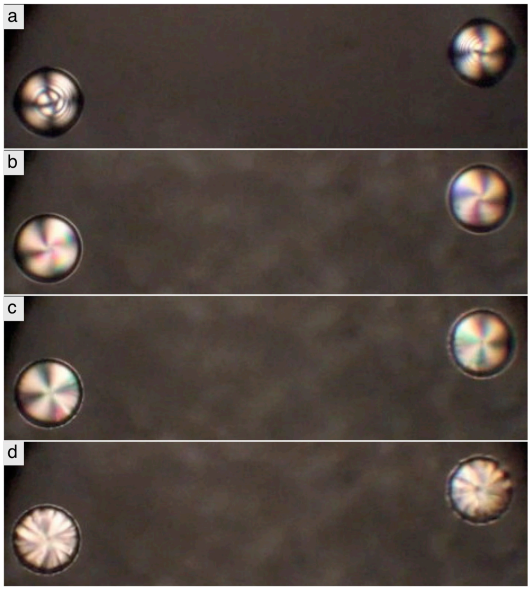

Fig. 6. Two shells going through the same transition as in Fig. 5. Note how the twist is in opposite directions in the two shells.

The spiral is always centered on the top of the shell and the first instance of textural change is always found in this regime. This can be understood as a result of the fact that the shell is not entirely symmetric: because of density mismatch between the aqueous phase and the liquid crystal (the latter having higher density), the inner droplet rises towards the top of the shell, making it thinner there and thicker at the bottom. The asymmetry can be verified by tilting the microscope by 90°, allowing observation "from the side" with respect to gravity. The top thus becomes the energy-minimizing location for the s =+1 defect that must develop upon the change to planar alignment [17] and it should also be the place of minimum energy barrier for the alignment change. After the phase transition the SmA texture is rotationally symmetric about the top of the shell, at which an s =+1 defect can indeed be identified, cf. Fig. 5h.

The origin of the alignment change seen upon approaching the N-SmA transition is not entirely obvious. The structure of F127 is quite different from classic low-molar-mass ionic surfactants such as CTAB or SDS, which clearly promote a homeotropic alignment in the liquid crystal. F127, in contrast, should be much less discriminative regarding director alignment and it may thus be the liquid crystal itself that prefers planar alignment in the smectic phase but homeotropic in the nematic. A possible reason for this could be the shell asymmetry: in the nematic phase a variation in shell thickness is problem-free for planar as well as homeotropic alignment, but in the smectic phase a homeotropically aligned asymmetric shell will contain a high number of layer edges, as the layers of the thick part of the shell not fitting in the thin part cannot close up (cf. Fig. 7). It may thus be preferable to adapt a basically planar alignment with focal conic defects, where the layers close up on a much more local scale into Dupin cyclides.

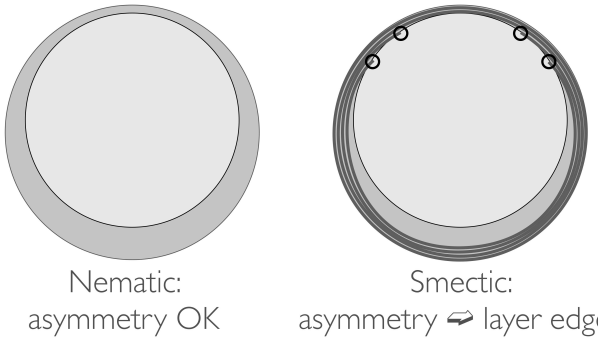

Fig. 7. Schematic illustration of the problem of asymmetry for a homeotropically aligned smectic shell.

Alternatively the change may be driven by the change in the hydrophilic-hydrophobic balance of F127 as the temperature is changed. Although the drastic change from micelles to unimers occurs substantially below the temperature of the alignment change, the increase of hydrophilicity of the F127 polymer on cooling is a continuous process that may play a role in the observed behavior. At high temperatures the difficulties for the PEO moieties to hydrogen bond with the water may lead them to prefer contact with the polar cyano group of the 8CB mesogens rather than the nonpolar aromatic core. A homeotropic alignment would then be promoted. As the solubility of F127 increases as we cool from the nematic to the smectic phase the PEO moieties get increasingly dissolved in the water phase instead, leaving the liquid crystal shell primarily in contact with the hydrophobic PPO moieties. These prefer contact with the aromatic cores, hence this situation favors a planar alignment. Further experiments on shells of a different *n*CB homologue, liquid crystalline over the temperature range considered but without a phase transition in that range, would be required to discriminate which of these scenarios is dominating. Such experiments are underway.

4. Conclusions

New and very interesting ways of studying and applying liquid crystals can be achieved using electrospinning and microfluidic generation of fluid shells. These are of interest for a variety of new applications and they also display a range of new fascinating physicochemical phenomena of more fundamental research character, the investigation of which has only begun. Among these may be mentioned the consequences of confinement on the liquid crystal inside the electrospun fibers, e.g. quantization of color of a cholesteric, and temperature dependent changes between planar and homeotropic alignment in the shells

Acknowledgments
We thank Liang-Yin Chu for very kind advice regarding the construction of the microfluidic set-up and Enzo Calò for assistance with the electron microscopy investigations.

References

1. D.H. Reneker, and A.L. Yarin, " Electrospinning jets and polymer nanofibers ", Polymer, 49, 10, 2387 (2008).
2. A. Greiner, and J.H. Wendorff, " Electrospinning: A fascinating method for the preparation of ultrathin fibres", Angew. Chem. (Int. Ed.), 46, p. 5670 (2007).
3. D. Li, and Y. Xia, " Electrospinning of Nanofibers: Reinventing the Wheel?", Adv. Mater., 16, p. 1151 (2004).
4. J.P.F. Lagerwall, J.T. McCann, E. Formo, G. Scalia and Y. Xia, “Coaxial electrospinning of microfibres with liquid crystal in the core”, Chem. Commun., 42, 5420 (2008).
5. E. Enz, U. Baumeister and J. Lagerwall, “Coaxial electrospinning of liquid crystal-containing poly(vinyl pyrrolidone) microfibers”, Beilstein J. Org. Chem., 5, DOI: 10.3762/bjoc.5.58 (2009).
6. E. Enz and J. Lagerwall, “Electrospun microfibres with temperature sensitive iridescence from encapsulated cholesteric liquid crystal”, J. Mater. Chem., 20, 6866 (2010).
7. A. Utada, E. Lorenceau, D.R. Link, P.D. Kaplan, H.A. Stone and D.A. Weitz, “Monodisperse double emulsions generated from a microcapillary device”, Science, 308, 537 (2005).
8. J. Selinger, M. Spector, and J. Schnur, " Theory of self-assembled tubules and helical ribbons", J. Phys. Chem. B, 105, 7157 (2001)
9. D. R. Nelson, “Toward a tetravalent chemistry of colloids”, Nano. Lett., 2, 1125 (2002).
10. J.P.F. Lagerwall, "Three facets of modern liquid crystal science", Habilitation thesis, Martin-Luther-Universität Halle-Wittenberg, Halle, Germany (2010).
11. H.-L. Liang, S. Schymura and J. P. F. Lagerwall, "Smectic Liquid Crystal Shells Produced by Coaxial Microfluidics", proceedings from the 38th Topical Meeting of the German Liquid Crystal Society, (2010).
12. M. Nakano, T. Teshigawara, A. Sugita, W. Leesajakul, A. Taniguchi, T. Kamo, H. Matsuoka, and T. Handa, "Dispersions of liquid crystalline phases of the monoolein/oleic acid/Pluronic F127 system", Langmuir, 18, 9283 (2002)
13. J. J. Escobar-Chávez, M. López-Cervantes, A. Naïk, Y. N. Kalia, D. Quintanar-Guerrero, A. Ganem-Quintanar, "Applications of thermoreversible Pluronic F-127 gels in pharmaceutical formulations", J. Pharm. Pharmaceut. Sci., 9, 339 (2006)
14. Y. Lin and P. Alexandridis, " Temperature-Dependent Adsorption of Pluronic F127 Block Copolymers onto Carbon Black Particles Dispersed in Aqueous Media", J. Phys. Chem. B, 106, 10834 (2002)
15. F. Dickert, A. Haunschild, and P. Hofmann, "Cholesteric liquid-crystals for solvent vapor detection - elimination of cross-sensitivity by band shape-analysis and pattern-recognition", Fresenius J. Anal. Chem., 350, 577 (1994)
16. C. L. Casper, J. S. Stephens, N. G. Tassi, D. B. Chase and J. F. Rabolt. "Controlling surface morphology of electrospun polystyrene fibers: Effect of humidity and molecular weight in the electrospinning process", Macromolecules, 37 573 (2004).
17. A. Fernandez-Nieves, V. Vitelli, A.S. Utada, D.R. Link, M. Marquez, D.R. Nelson, and D.A. Weitz, "Novel defect structures in nematic liquid crystal shells", Phys. Rev. Lett., 99, 157801 (2007)